EurJIC
European Journal of Inorganic Chemistry

Research Article
doi.org/10.1002/ejic.202300649

Chemistry Europe
European Chemical Societies Publishing

www.eurjic.org

Chirality Generated by Hindered Rotations in Platinum(II)-Pyridine Complexes

Sergio Stoccoro,*[a, b] Alessandro Sini,[a] Giacomo Senzacqua,[a, b] Luca Maidich,[a] Fabrizio Ortu,[c] and Antonio Zucca*[a, b]

The reaction of *trans*-[Pt(DMSO)$_2$MeCl] with 2-alkylsubstituted pyridines py^R affords a series of complexes of the type [Pt(py^R)(DMSO)MeCl]. These complexes are rare examples of organometallic square-planar complexes having four different ligands. Of the three possible geometric isomers, only the *trans*(N,S)-[Pt(py^R)(DMSO)MeCl] was observed in solution and isolated in the solid state. However, the lack of chirality typical to square planar geometry can be resolved in several ways one of which is described in this paper. ^{1}H NMR studies reveal diastereotopicity of the DMSO methyls, as well as the CH_2 protons in the ethyl- and neopentyl-pyridine complexes and the methyls in the isopropyl-pyridine derivative. This observation can be ascribed to restricted rotations around the Pt–N bond, thus resulting in the presence of planar chirality for these complexes. Additionally, large downfield shifts in the ^{1}H NMR spectra of the α C–H protons in the pyridine substituents suggested the presence of Pt···H–C interactions, confirmed *via* single crystal X-ray studies in the case of the isopropyl complex [Pt(py^{ip})(DMSO)MeCl] (**4**), which shows an apical Pt···H interaction with a short 2.585 Å distance. DFT calculations shed light into the stability of these complexes and the influence of the pyridine-substituent on their chiral configuration.

Introduction

Pyridine complexes of noble metals have been investigated for a long time.[1] In particular, platinum(II) complexes have been the subject of extensive research in different fields, from biomedicine to photochemistry. Various studies concern the kinetic aspects of their syntheses and their reactivity: as an example, the complex *trans*-[Pt(py)$_2$Cl$_2$] has been chosen as the standard substrate for setting up a scale of nucleophilic ligand substitution in square planar complexes.[2] Furthermore, platinum(II) cyclometalated complexes derived from 2-arylpyridines have shown to be strongly emissive with long luminescent lifetimes,[3] and some platinum(II)-pyridine complexes have attracted great attention due to their potent biological activity. As an example, picoplatin, *i.e.* the complex *cis*-[Pt(NH$_3$)(2-methylpyridine)Cl$_2$], has been evaluated in Phase I and II clinical trials for the treatment of a range of tumors, including prostate, lung, and colon cancer.[4]

In 1996 Romeo and co-workers investigated the solution behavior of the useful organometallic starting material *trans*-[Pt(DMSO)$_2$MeCl], showing that this labile species exists in solution as a mixture of *cis*- and *trans*- geometric isomers, as well as their corresponding aquo complexes *cis*-[Pt(DMSO)(H$_2$O)MeCl] and *trans*-[Pt(DMSO)(H$_2$O)MeCl]. The lability of the DMSO ligand was exploited to study the substitution reaction with of a series of nitrogen ligands (L_N) to afford the monosubstituted complexes [Pt(L_N)(DMSO)MeCl] (Figure 1). These are rare square-planar organometallic complexes featuring four different ligands, that may exist in three different stereoisomers: *trans*(N,S) (**I**), *trans*(N,C), (**II**) and *trans*(N,Cl), (**III**).

Depending on the steric properties of the nitrogen ligand L_N, either isomers **I** or **II** were formed and isolated, whereas isomer **III** was never observed.[5] In further work, Romeo, Monsù Scolaro and co-workers showed that isomer **II** (*trans*(N,C)) is the kinetic product, subsequently isomerizing into the more stable *trans*(N,S) isomer **I**. In addition, useful criteria for the NMR distinction between the isomers were given, based on $^2J_{Pt–H}$ and $^3J_{Pt–H}$ coupling constants for coordinated methyl and DMSO ligands.[6]

One important aspect emerged from this study is that bulky substituted pyridine ligands induced slow rotation around the Pt–N bond, introducing a chirality element in the complexes. This important point (*i.e.* chirality of square planar complexes) has not received a lot of attention outside of Romeo and Monsù Scolaro's work and it is often overlooked, especially when achiral ligands are used. In the case of platinum complexes with nitrogen ligands, chirality has been widely treated for octahe-

[a] Prof. S. Stoccoro, Dr. A. Sini, Dr. G. Senzacqua, Dr. L. Maidich, Prof. A. Zucca
Dipartimento di Scienze Chimiche
Fisiche, Matematiche e Naturali
Università degli Studi di Sassari
via Vienna 2
07100 Sassari (Italy)
E-mail: stoccoro@uniss.it
zucca@uniss.it

[b] Prof. S. Stoccoro, Dr. G. Senzacqua, Prof. A. Zucca
Consorzio Interuniversitario
Reattività Chimica e Catalisi (CIRCC)
Bari (Italy)

[c] Dr. F. Ortu
School of Chemistry
University of Leicester
University Road
Leicester, LE1 7RH (UK)

Supporting information for this article is available on the WWW under https://doi.org/10.1002/ejic.202300649

Research Article
doi.org/10.1002/ejic.202300649

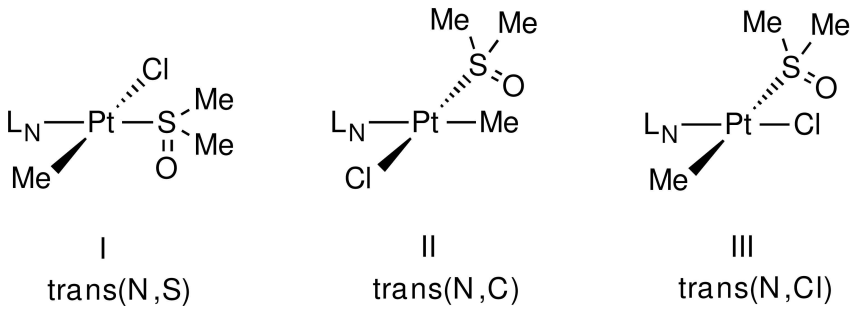

Figure 1. Stereoisomers of [Pt(L_N)(DMSO)MeCl] complexes.

dral Pt(IV) derivatives,[7] but for square planar Pt(II) complexes attention has been restricted to special cases, such as helical chirality, restricted rotations of bulky ligands, or boat-like conformations of six-membered chelated ligands, in addition to the obvious cases of coordination of chiral ligands.[8]

Furthermore, the situation regarding the stereodescriptors for axial chirality, planar chirality and helicity has been often treated in different and sometime confused ways.[9]

Among the ample series of nitrogen derivatives described in Romeo's papers, the pyridine complexes attracted our interest: the less hindered ligands *i.e.* the unsubstituted pyridine (py) and 2-methylpyridine (py^{Me}) gave, exclusively the *trans*(N,S) isomers [Pt(py)(DMSO)MeCl], **1**, and [Pt(py^{Me})(DMSO)MeCl], **2**. The reaction outcome is dependent on the steric properties of the nitrogen ligands, hence the bulkier di-substituted 2,6-dimethylpridine (py^{Me2}) gave the *trans*(N,C)-[Pt(py^{Me2})(DMSO)-MeCl] isomer, whereas 2-phenylpyridine (py^{Ph}) gave a mixture of *trans*(N,S) and *trans*(N,C) [Pt(py^{Ph})(DMSO)MeCl] complexes.

In the last decades our research group has undertaken a systematic study of square-planar d^8 metal complexes with pyridine-derived ligands,[10] with a particular focus on the influence of substituents on the reactivity and properties of resulting complexes. These studies are part of a broader topic, in which the influence of alkyl substituents adjacent to the nitrogen in pyridine-like ligands constitute a little but significant part, especially with regards to the chemistry of platinum(II).[11]

The [Pt(py^R)(DMSO)MeCl] complexes described by Romeo and co-workers have attracted our interest for their unique stereoisomerism. The role played by the R substituent on the pyridine ligand in these complexes is crucial in creating the basis for a planar chirality. The hindered rotation around the Pt–N bond, connected to the bulkiness of R, differentiates the upside and downside positions of the substituent, generating a couple of enantiomers. For this reason we decided to extend the study to 2-alkyl-substituted pyridines (py^R) which feature a wide range of sterical hindrance on the carbon in 2-position, comparing py and py^{Me} (R=H and CH_3) with 2-ethylpyridine (py^{Et}, R=CH_2CH_3), 2-*iso*propylpyridine (py^{ip}, R=$CH(CH_3)_2$) and 2-*tert*-butylpyridine (py^{tb}, R=$C(CH_3)_3$).

In this context we report here the synthesis and description of a series of Pt(II) chiral organometallic complexes with 2-alkylpyridines, [Pt(py^R)(DMSO)(Me)Cl], where the presence of the substituent in the pyridine ring generates a hindered rotation around the Pt–N bond inducing planar chirality on the complex. Furthermore, the conformation of the complex is stabilized by an intramolecular Pt···H–C interaction, which has been investigated and analyzed.

Results and Discussion

This work is focused on the comparison of substituted pyridine ligands with an increasing degree of substitution on the carbon atom of the substituent in the 2-position (Figure 2), where this alpha-carbon carries different substitution patterns: 1) three hydrogens (py^{Me}); 2) two hydrogens and one methyl (py^{Et}); 3) one hydrogen and two methyls (py^{ip}); 4) no hydrogens and three methyls (py^{tb}). In addition, in order to expand our understanding of this class of complexes, we investigated two further ligands featuring slightly different substituents: 2 neopentyl-pyridine (py^{np}) and 2-vinyl-pyridine (py^{vi}).

The bulkiness of the substituent is crucial for the coordinating behavior of the ligands and, as shown below, in directing the properties of the resulting complexes. The substitution of hydrogens with methyls is not a trivial modification. It has been observed that substituting hydrogen atoms, positioned close to the metal center, with methyl groups, may cause a drastic change in the properties of the corresponding complexes. Examples of this are Pt(II) complexes with cyclometalated 6-benzylsubstituted 2,2′-bipyridines where unexpected metal-hydrogen interactions significantly changed the behavior of the resulting Pt(II) complexes.[12]

Some of the ligands studied are not commercially available; in particular, 2- *iso*-propylpyridine (py^{ip}) and 2-*tert*-butylpyridine (py^{tb}) were synthesized following a procedure which allows the construction of the pyridyl ring starting from the corresponding nitrile through cyclotrimerization with acetylene in the presence of the cobalt Bonneman catalyst (see experimental).[13]

The platinum(II) precursor used in this work, *trans*-[Pt-$(DMSO)_2MeCl$], is a well-known organometallic starting material, often compared to the more electron-rich *cis*-[$Pt(DMSO)_2Me_2$] and the more electron-poor *trans*-[$Pt(DMSO)_2Cl_2$].[14,15]

The reaction with the pyridine ligands was conducted in dichloromethane solution at room temperature allowing the isolation of complexes *trans*(N,S)-[Pt(py^{Et})(DMSO)MeCl] (**3**), *trans*-(N,S)-[Pt(py^{ip})(DMSO)MeCl] (**4**), *trans*(N,S)-[Pt(py^{np})(DMSO)MeCl] (**6**), and *trans*(N,S)-[Pt(py^{vi})(DMSO)MeCl] (**7**), all obtained in high yields (Scheme 1). In the case of the *tert*-butyl substituted

Research Article
doi.org/10.1002/ejic.202300649

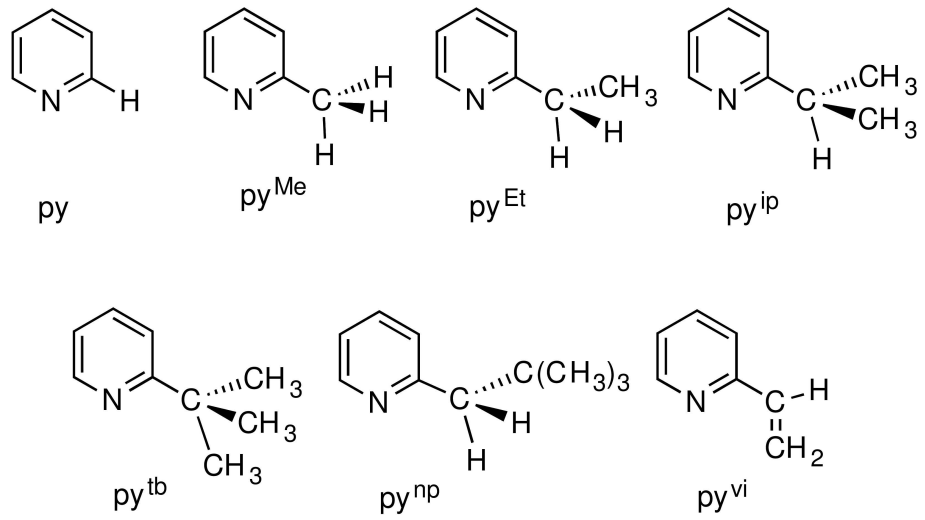

Figure 2. Pyridine ligands compared and investigated in this work.

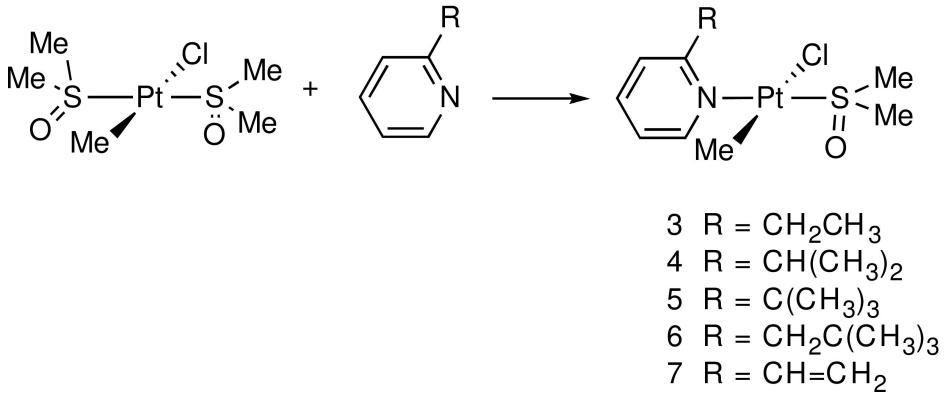

Scheme 1. Synthesis of complexes **3**–**7**.

ligand, the corresponding complex *trans*(N,S)-[Pt(py^{tb})(DMSO)-MeCl] (**5**) was obtained in low yields, in mixture with the starting complex *trans*-[Pt(DMSO)$_2$MeCl], likely due to the steric bulkiness of the ligand, whereas complex **7** rapidly converts into the cyclometalated complex *trans*(N,S)-[Pt(py^{vi}-H)(DMSO)Cl] (**8**) upon loss of methane.

In all cases, only the mono-substitution product was isolated or observed in solution, even when operating with a two-fold excess of ligand, thus indicating that the second DMSO ligand becomes less labile after the substitution of the first one.[5] This may be due to a strengthening of the Pt–S bond after the first substitution reaction, likely due to a stronger π-back donation of the Pt atom in the mono-solvated complexes compared to the bis-solvated starting material, in which retro-donation was distributed towards two DMSO ligands.

Complexes **3**–**7** were characterized *via* elemental analysis, IR and NMR spectroscopies, and, in the case of **4**, by single-crystal X-ray diffraction and DFT methods. In all cases the ^{1}H NMR spectra showed only the presence of the *trans*(N,S) isomer (isomer **I**, Figure 1). With the exception of complex **5** (py^{tb}), conversions to the target complexes are almost quantitative, though the values given in the experimental section are lower (*ca.* 75–85 %) as they refer to isolated yields, which are affected by the high solubility of these species. In the case of the py^{tb} ligand the yield is lower, likely due to the bulkiness of the *tert*-butyl substituent and for this reason complex **5** was not isolated in pure form, but rather as part of a mixture with the reagents.

The ^{1}H NMR spectra of **3**–**7** show the expected signals for the proposed geometry: *i.e.* singlets with satellites integrating for one DMSO ligand and one methyl group with Pt–H coupling constant in line with a *trans* S–Pt–N ($^3J_{Pt–H}$ = 26–27 Hz) and *trans*-CH$_3$–Pt–Cl coordination ($^2J_{Pt–H}$ = *ca.* 83 Hz). These data rule out the other two isomers, considering as an example the *trans*(C,N) isomer where a $^2J_{Pt–H}$ = *ca.* 75 Hz is expected for the Pt–CH$_3$ protons.[5]

It is noteworthy that the DMSO methyl protons in **3**–**7** give rise to two singlets with satellites (each integrating 3 protons) (*e.g.* **4** (C_6D_6): 3.09 ($^3J_{Pt–H}$ = 26.8 Hz); 3.05 ($^3J_{Pt–H}$ = 26.3 Hz)) showing that they are diastereotopic, and, consequently, that the complexes are chiral. Concurrently, the CH$_2$ protons in **3** and **6**, and the *iso*-propyl methyls in **4** are diastereotopic as well.

Research Article
doi.org/10.1002/ejic.202300649

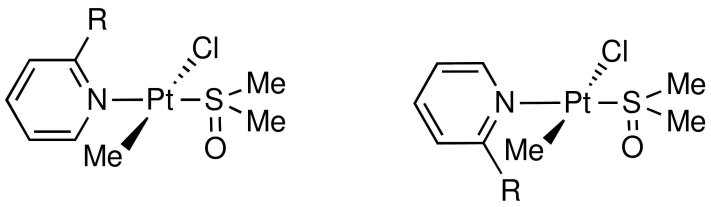

Figure 3. Couple of enantiomers generated by hindered rotation around the Pt–N bond.

In the case of complexes **3** and **4** the splitting of the DMSO signals is not observed in CD_2Cl_2 solution, likely due to a small separation of the singlet signals. At variance, the two methyls of the isopropyl substituent in **4** are well separated also in CD_2Cl_2 solution (δ 1.39 and 1.33).

The presence of diastereotopic methyls is related to the presence of the pyridine substituent in 2-position and should be attributed to a hindered rotation on the NMR time scale around the Pt–N bond (see Figure 3), generating a couple of enantiomers.

Three types of hindered rotations may be considered: rotations around the Pt–S bond, the Pt–N bond and the C–C bond of the pyridine substituent.

Let us take the complex with py^{ip} as an example. The hindered rotation of DMSO (rotation around the Pt–S bond) would make the DMSO methyls different but not those of *iso*-propyl group, due to the rotation around the Pt–N bond which interconverts the positions; the hindered rotation of the *iso*-propyl substituent does not change the situation in the presence of a free rotation of the pyridine ligand, which interconverts the methyls. For these reasons, we deem that the hindered rotation responsible for the chirality is that of the pyridine ligands, *i.e.* the hindered rotation around the Pt–N bond. A DFT dynamic analysis on this point is reported later.

A further aspect revealed by the ^{1}H NMR spectra of these complexes is the strong deshielding of the C–H proton signals in α on the pyridine substituents with respect of the free ligand. This is particularly evident for the C–H of the *iso*-propylpyridine, with a coordination shift $\Delta\delta = 1.43$ ppm (δ 3.06 in the free ligand; 4.49 in **4**). The downfield shift is observed also for **2** and **3**, but to a lesser extent ($\Delta\delta$ = ca 0.5–0.6 ppm), likely due to mediation between three and two hydrogens, respectively. In the case of complex **6** a deshielding of *ca.* 1.3 ppm is observed (δ = 2.42 (free py^{np}), 3.71 (complex **6**)).

As for complex **7**, 2-vinylpyridine is structurally different form the other ligands. The study showed that in this case the coordination reaction is extremely fast: after addition of 2-vinylpyridine to [Pt(DMSO)$_2$MeCl], **7** is formed almost immediately. However, **7** quickly converts into the cyclometalated complex **8**, following a rapid room-temperature C–H bond activation with liberation of methane (Scheme 2).

An NMR analysis of complex **7** is only achievable by rapidly isolating the complex at low temperature and promptly recording the ^{1}H NMR spectrum: the spectrum shows that the vinylic α proton is extremely deshielded (from 6.71 ppm in the free ligand to 7.99 ppm in **7**, $\Delta\delta = 1.28$ ppm), also showing a coupling with the ^{195}Pt nucleus $J_{Pt-H} = 11.3$ Hz.

These data again indicate the presence of a possible Pt···H–C interaction, but the study of the complex is difficult due to the rapid cyclometalation of the complex to afford complex **8**. The latter reaction is interesting, because the activation occurs rapidly at room temperature. In addition, the C–H bond engaged in the Pt···H–C interaction is not involved in the reaction, which is selective towards the β-vinylic hydrogens which are supposed to be located far to the metal, so that a rotation of the substituent is needed for the C–H bond activation. The synthesis of **8** has been previously described by some of us starting from [Pt(DMSO)$_2$Me$_2$] and unambiguously ascertained by the resolution of the structure of successive reaction products.[16] In that case, however, we did not observe an easy metalation at room temperature.

The downfield shift observed for complexes **2**–**7** is not unprecedented. Similar downfield shifts have been often observed in square-planar complexes when a C–H group of a ligand is located above a square-planar d^8 metal center, being indicative of some kind of interaction with the metal (Figure 4). These interactions have been called and classified in several ways, such as agostic, pregostic, pre-agostic, *etc.* (see later in the paper), so we decided to investigate one of the complexes

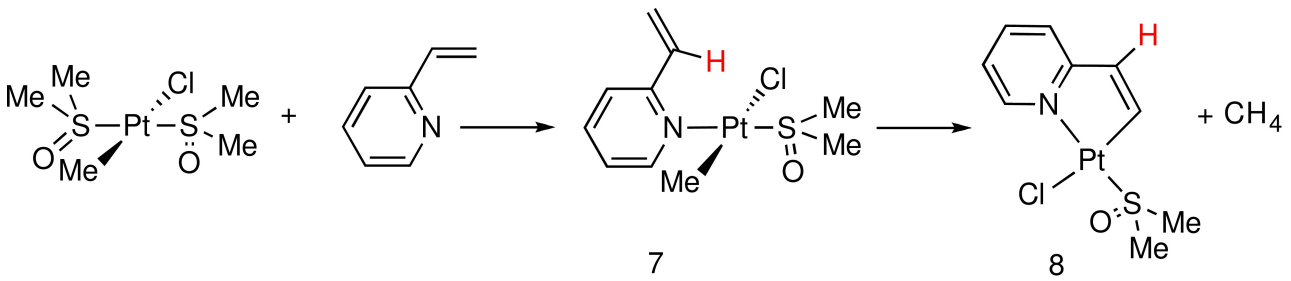

Scheme 2. Behavior of 2-vinylpyridine.

Research Article
doi.org/10.1002/ejic.202300649

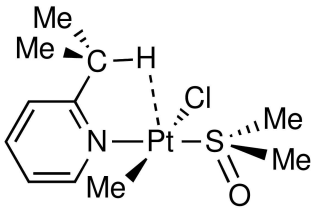

Figure 4. Pt—HC interaction in complex **4.**

in detail in order to shed light into its structural properties. Complex **4** was chosen for the study, having only one hydrogen in the α-carbon of the substituent.

Compound **4** crystallizes in the monoclinic space group $P2_1/n$, displaying a regular square planar geometry around the Pt center [N(1)–Pt(1)–C(9) 87.58(14)°, N(1)–Pt(1)–Cl(1) 88.82(8)°, Cl(1)–Pt(1)–S(1) 93.43(4)°, S(1)–Pt(1)–C(9) 90.18(12)°], which sits almost perfectly on the plane described by the four ligands [Pt···N(1) C(9) S(1) Cl(1) = 0.0206(12) Å]. The Pt-methyl distance [2.045(5) Å] is consistent with previously reported compounds.[11d,17] The molecular structure confirms the presence of a single isomer featuring the pairs methyl-chloride and pyridine-DMSO as *trans*-oriented ligands [N(1)–Pt(1)–S(1) 176.69(8)°, C(9)–Pt(1)–Cl(1) 176.39(12)°]. There are numerous mixed methyl-chloride complexes supported by nitrogen donors reported in the literature; nonetheless, in all cases the methyl ligand is positioned *cis* to a chloride due to the presence of bidentate nitrogen ligands.[17a–c] Conversely, in the case of **4** isomerization is possible because of the monodentate nature of all ligands involved in the metal coordination sphere, and, to the best of our knowledge, complex **4** is the first example of a structurally authenticated Pt(II) complex supported by a nitrogen donor exhibiting this *trans*-type arrangement.[17d] This coordination motif is also reminiscent of the complex *trans*-$[Pt(SMe_2)MeCl]_2$ reported by Puddephatt and co-workers, though its molecular structure also contains *cis*-$[Pt(SMe_2)_2Cl_2]$ with an occupancy of approximately 15%.[18] It is noteworthy that there are several reports of structurally authenticated Pd-aryl complexes containing aryl and halide ligands in a *trans* arrangement.[17d,19]

Interestingly, atom H(6) belonging to the *iso*-propyl substituents occupies an apical position directly above the Pt center, sitting at 2.585 Å and thus hinting at the presence of an interaction with the C–H bond of C(6) [Pt(1)···C(6) 3.263(3) Å] (see Figure 5). It is noteworthy that, although hydrogen atoms have all been positioned using a riding model, a peak was clearly visible in the diffraction map in the position occupied by H(6) (see SI, Figure S1). Long range π-π stacking interactions [3.443 Å] can be observed between the pyridyl ligands of neighboring complex molecules, involving atoms C(2), C(3) and C(4).

DFT Calculations

A series of DFT calculations were performed to further investigate the observed results, in particular we concentrated our attention on the comparison between complexes **1** and **4**, in order to highlight the influence of the substituent.

We started our analysis finding the gas phase minima for the coordination isomers following the schemes depicted in Figure 1. This preliminary work confirmed isomer **I**, with a *trans*(N,S) arrangement, as the one with the lowest energy both for **1** and **4**. As for complex **4**, rotation of the *iso*-propyl substituent was also considered, leading to rotamers **4a** (the one found in the X-ray analysis) having the C–H bond pointing towards the metal, and **4b**, having the *iso*-propyl methyls above the metal center (Figure 6). Noteworthy, both rotamers of complex **4** follow the same trend having the *trans*(N,S) isomer as the most stable conformation (see Table 1). According to our data, the less stable isomer for both ligands is the *trans*(N,C) one, *i.e.* the kinetic product of the reaction according to Romeo and co-workers. Isomer **III**, though never detected in solution, appears to be slightly more stable than isomer **II**. The

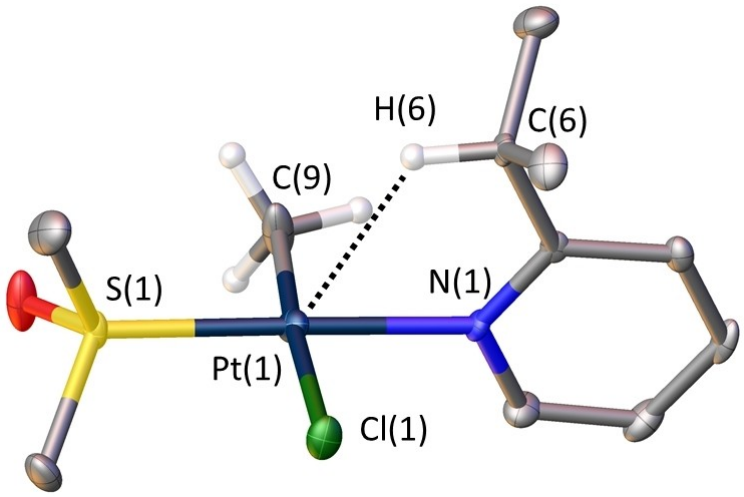

Figure 5. Molecular structure of **4** with ellipsoids set at 30% probability level. Hydrogen atoms have been omitted for clarity with the exceptions of those belonging to methyl ligand C(9) and methine group of the *iso*-propyl substituent on the pyridyl ligand C(6).

Research Article
doi.org/10.1002/ejic.202300649

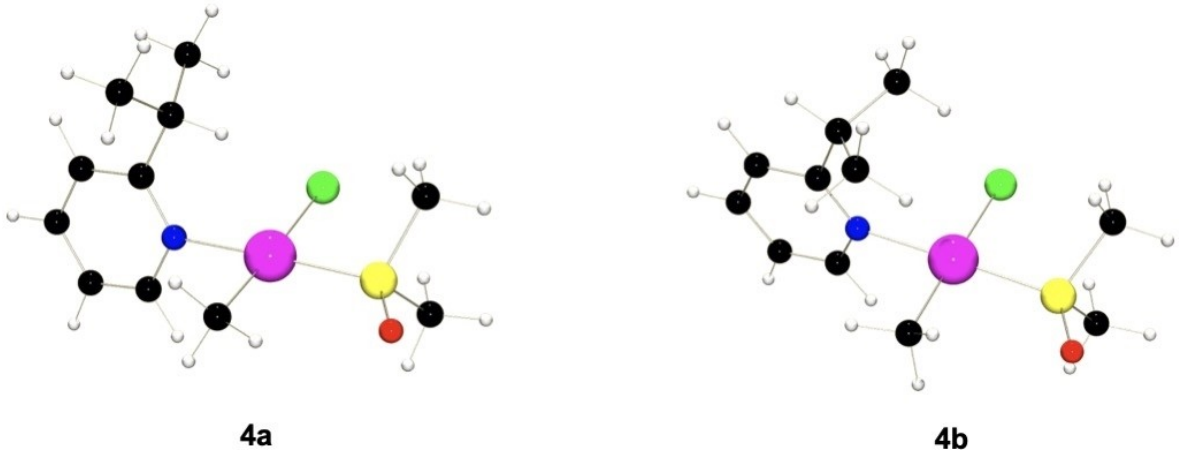

Figure 6. Equilibrium geometries of the two rotamers originated from the rotation of the *iso*-propyl on the pyridine in complex **4**.

Table 1. **A**) ZPE corrected ΔH and ΔG values, in kJ/mol, for the different isomers of [Pt(py)(Me)(DMSO)] and complex **4**. The lowest energy isomer was taken as reference. **B)** ZPE corrected ΔH and ΔG activation values, in kJ/mol, associated to the rotation of the DMSO, pyridine and *iso*-propyl groups in complexes **1**, **4a** and **4b**.

A		ΔH			ΔG	
L_N (complex)	py (**1**)	py^{ip} (**4a**)[a]	py^{ip} (**4b**)[a]	py (**1**)	py^{ip} (**4a**)[a]	py^{ip} (**4b**)[a]
trans(N,S) (I)	0	0	0[b]	0	0	0[b]
trans(N,C) (II)	14.0	13.0	13.5	14.2	13.4	13.4
trans(N,Cl) (III)	12.2	9.2	11.0	9.9	7.5	10.5
B		ΔH≠			ΔG≠	
Rotation of L_N	py (**1**)	py^{ip} (**4a**)	py^{ip} (**4b**)	py (**1**)	py^{ip} (**4a**)	py^{ip} (**4b**)
Pt–S (L_N = DMSO)	40.0	37.8	37.1	43.6	42.9	43.1
Pt–N (L_N = py)	9.4	78.3	–	15.6	87.0	–
C–C[c] (L_N = py^{ip})	–	36.4	19.0	–	41.6	22.8

[a] **4a** indicates rotamer where CH of C_{ipso} is on top of Pt while **4b** identifies the one with two CH from the methyl groups on top of Pt; [b] ΔH: **4b** is 17.4 kJ/mol less stable than **4a**; ΔG: **4b** is 18.8 kJ/mol less stable than **4a**; [c] rotation of the *iso*-propyl substituent in **4** around the $C_{2(py)}$–C_{ip} bond.

stabilization energy of isomer **I** *vs* **II** amounts to *ca* 13–14 kJ/mol. The two isomers of complex **4**, **4a** and **4b**, differ by ca. 19 kJ/mol; **4a**, *i.e.* the one with the α C–H of the *iso*-propyl pointing towards Pt centre being the one with the lowest energy.

The activation energies for some bond rotations were also analyzed. Rotation of the DMSO ligand showed a minimum energy for the rotamer having the oxygen close to methyl ligand and, consequently, the DMSO methyls oriented towards the chloride. The most interesting data are related to the rotation of the pyridine ligands: due to the presence of the *iso*propyl substituent, rotation of py^{ip} around the Pt–N bond in **4** is significantly higher than that of unsubstituted pyridine in **1** ($\Delta G^{\neq}$ 87.0 vs 15.6 kJ/mol), ascribing the chirality of complex **4** to this restricted rotation.

The last line in Table 2 refers to the rotation of the *iso*-propyl substituent around the C–C pyridine-*iso*-propyl bond. $\Delta G^{\neq}$ activation data show that the **4a** rotamer bearing the Pt···H–C interaction is more stable by 18.8 kJ/mole than **4b**. The Gibbs' free activation energy value for the rotation of *iso*-propyl substituent is 41.6 kJ/mol, starting from **4a**.

Comparison of the X-ray structure with the lowest energy isomer obtained via DFT calculations show a good agreement in bond distances and angles. Mean absolute error (MAE) considering all bonds is 0.02 Å, whilst for angles it is 0.75 degrees; in both cases MAEs are slightly higher when the Pt metal center is included.

Comparison of complex **4** (**4a** rotamer) with complex **1** (Figure 7) allows us to highlight the changes to the geometry linked to the presence of the *iso*-propyl substituent. Unsurprisingly, the differences in bond distances and angles between the two complexes are in the same range of the experimental error. Worthy of note is the dihedral angle associated to the rotation around the Pt–N bond: the presence of the *iso*-propyl substituent on the pyridine in complex **4** forces the heteroaromatic ligand in a more perpendicular position relatively to the coordination plane.

Research Article
doi.org/10.1002/ejic.202300649

Table 2. Comparison of selected geometrical parameters for complex **4**, X-ray structure and lowest energy isomer were considered.

Bond	**4** X-ray	**4a** DFT	**1** DFT
Pt–N	2.0600	2.0666	2.0561
Pt–CH3	2.0450	2.0462	2.0443
Pt–S	2.1860	2.2148	2.2172
Pt–Cl	2.4070	2.4374	2.4344
Pt–H(C_{ipso})	2.5850	2.4934	–
Angles			
N–Pt–CH_3	87.60	88.13	89.59
CH_3–Pt–S	90.20	92.26	90.95
S–Pt–Cl	93.43	90.40	90.15
Cl–Pt–N	88.82	89.23	89.31
N–Pt–S	176.69	177.48	179.06
Cl–Pt–CH_3	176.40	177.34	178.75
Dihedrals			
C_2–N–Pt–Cl	−81.60	−72.31	−43.55
O–S–Pt–CH_3	16.00	1.40	−0.33

Selected geometrical parameters for complex **1** and **4** are visible in Table 2.

In order to have insights into the Pt···H interaction evidenced in complex **4**, we also evaluated the *ZPE corrected ΔG* values in CH_2Cl_2 solution (SMD approximation) for the overall coordination reactions involving pyridine and *iso*-propylpyridine, (Figure 8):

In this way, after subtracting the same reagents and products we may evaluate the relative stability of complexes **1** and **4**.

ΔG values are in agreement with an easy substitution reaction to give stable Pt-pyridine complexes: comparison of the calculated *Δ*G values for **1** and **4** indicates that the unsubstituted pyridine gives a more stable complex than *iso*-propylpyridine (*ΔG* −29.61 vs −24.06 kJ/mol), difference almost completely ascribable to entropic contributions, likely due to restricted movements in the coordinated pyridine substituent.

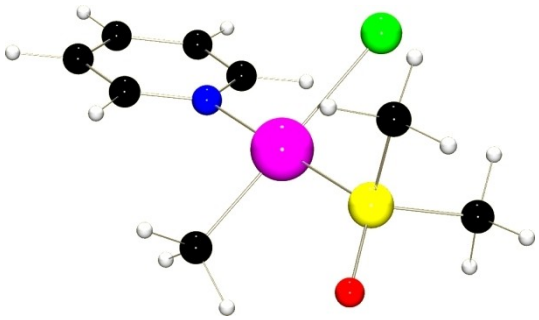

Figure 7. Equilibrium geometry for complex **1**.

Overall, it results that the presence of the substituent reduces the coordinating ability the py^{ip} ligand, but, once coordinated, the presence of a Pt···HC interaction results in a minimum of potential energy, stabilizing a chiral configuration of the complex.

Overall, the chiral configuration is strictly connected to the presence of the pyridine substituent, which greatly enhances the rotational barrier around the Pt–N bond (ΔG 87.0 kJ/mol in **4** vs only 15.6 kJ/mol in **1**), also in connection with the relative stabilization due to the Pt—H–C interaction.

Planar Chirality of the complexes

Overall, it is evident that the hindered rotation about the Pt–N bonds, together with the non-symmetric nature of the pyridines, generate a planar chirality situation.

Chirality in square planar complexes may be originated in several ways. The description is clear when chiral ligands are coordinated but becomes shadowy when chirality derives from hidden rotations around single bonds. Two classical cases are restricted rotations of a bulky ligand around the metal-donor bond and chelation of non-planar ligands. No common conventions have been adopted by inorganic chemists, and different stereodescriptors for diverse types of chirality, as axial chirality, planar chirality, and helicity, have been sometimes disorderly used.[9]

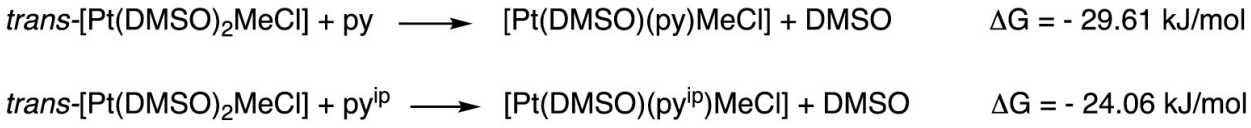

		Solvent CH_2Cl_2 (SMD approximation)	
		ΔH (kJ/mol)	ΔG (kJ/mol)
Complex **1**	py	-30.69 kJ/mol	-29.61 kJ/mol
Complex **4**	py^{ip}	-29.63 kJ/mol	-24.06 kJ/mol

Figure 8. Overall reaction for the synthesis of **1** and **4** in the gas phase with ZPE corrected ΔG values.

Research Article
doi.org/10.1002/ejic.202300649

Stereogenic elements are structural models ideated by chemists to assign the configuration by means of configurational descriptors (*e.g.* R,S or P,M). It is therefore not surprising that the identification of the stereogenic element may be sometimes ambiguous. This happens when the geometrical characteristics of a stereogenic element meet the definitions given for two different elements: in some cases, such as those described in this paper, plane and axis features are not so different (see Figure 9).

In our case we would be in favour of identifying a stereogenic plane for our compounds (the square-planar coordination plane), and describe these complexes in terms of planar chirality. Planar chirality refers to stereoisomerism resulting from the arrangement of out-of-plane groups with respect to a chirality plane, so it fits perfectly to our situation.

Following the treatment given by Lanfranchi and co-workers[9] we identify the CIP (Cahn-Ingold Prelog) priority of the ligands *cis* to the pyridine: in this case Cl vs methyl. As depicted in Figure 9, if the torsion angle τ((RCN)-Pt–Cl) is negative (left-handed helix) the chirality term is *M*, otherwise it is P.

Pt···H–C interaction

Chirality of this series of complexes may also be related to the presence of the Pt···H interaction suggested by NMR data and revealed in complex **4** by the X-ray analysis. Undoubtedly, the bulkiness of the substituent on the pyridine ring restricts the rotation of the pyridine ligand, but the presence of a Pt···H interaction may have a role in the stabilization of the conformer and, hence, on the enhancement of the rotational barrier. The interaction of a square-planar d^8 metal and a C–H group located above the metal is a longstanding and still non completely understood topic.

According to the literature, square-planar d^8 transition metal complexes may display different types of attractive and repulsive M···H–C interactions; several names and descriptions have been given by different authors but, overall, the interactions may be classified into four different types: i) repulsive anagostic 3c–4e, ii) attractive hydrogen-bond 3c–4e, iii) attractive 3c–2e preagostic and iiii) attractive 3c–2e σ-agostic interactions.[20] The interpretation of the downfield or upfield shifts in the NMR spectra of the hydrogen involved in the interaction, often used for a tentative interpretation, has been shown to be dubious, and several methods were proposed in order to understand the nature of this interaction. High pressure IR and diffraction studies revealed that square-planar d^8 complexes may display local Lewis acidity of the metal atom, providing "the electronic prerequisites to establish weakly attractive 3c–2e M···H–C agostic interactions".[20]

During the preparation of this manuscript Echeverrìa and Alvarez published a paper where several types of bonds were investigated and commented.[21] The authors analyzed the interpenetration between spheres of electron density (defined by van der Waals and covalent radii): when two atoms are involved in a bonding interaction, the outermost spheres of electron density interpenetrate to a greater or lesser extent depending on the strength of the interaction.

In a bond (or interaction) between atoms A and B, the penetration may be measured by means of a *p* index, defined as

$$p_{AB} = 100\frac{v_A + v_B - d_{AB}}{v_A + v_B - r_A - r_B} \quad (1)$$

where v_A and v_B are the van der Waals radii of atoms A and B, d_{AB} is the distance between the nuclei, r_A and r_B correspond to the covalent radii.

In the case of covalent bonding $p_{AB} = 100\,\%$, while in Van der Waals interactions, where there is no interpenetration $p_{AB} = 0\,\%$. The method is independent of the size of the interacting atoms: values around zero correspond to Van der Waals interactions, and values of approximately 100 correspond to a single covalent bond.

On the basis of covalent and Van der Waals radii reported by Echeverrìa and Alvarez we calculated the p values from the RX structure and for the DFT optimized structure (both in the gas-phase and CH_2Cl_2 solution, Table 3)

The last row of the table shows the p_{MH}-p_{MC} difference, which provides another perspective to set the interaction between the metal center and the C–H bond. According to this parameter, we would be about halfway between a C–H bond co-ordination and a hydrogen bond, but considering the M–H–C bond angle (approx. 125°) we are more towards the former case, but it is worth to remember that the system is constrained by the bond angles in the pyridine ligand.

It is noticeable that some bonds present a p_{AB} value greater than 100 %, likely due to the fact that polar covalent bonds are usually shorter than pure covalent bonds, for which a 100 % value is expected.

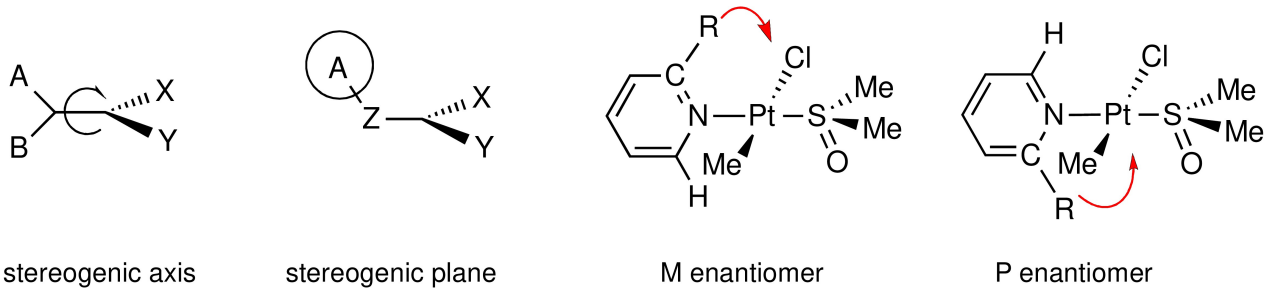

Figure 9. Comparison between stereogenic axes and planes; M and P enantiomers for complexes **2**–**7**.

Research Article
doi.org/10.1002/ejic.202300649

Table 3. p values for complex **4**, calculated from the structural and DFT data.

	X ray structure	DFT gas phase	DFT CH_2Cl_2 solution
Pt–N	100.11	99.76	99.84
Pt–CH_3	103.76	103.70	110.06
Pt–S	112.15	110.06	110.53
Pt–Cl	98.27	96.51	95.6
Pt–H (*ipso*)	49.53	54.55	54.91
PtC(*ipso*)	41.04	41.09	41.48
p_{MH}–p_{MC}	8.49	13.46	13.43

In conclusion, at this point we may assume that a stabilizing Pt···H–C interaction is present in complex **4**, as well as the other complexes reported in this paper: this interaction contributes to the stabilization of a chiral configuration, but the real nature of this interaction still remains to be further analyzed and disclosed.

Conclusions

In conclusion, we have shown that Pt(II) complexes with 2-alkylsubstituted pyridines (py^R) having four different ligands, such as [Pt(py^R)(DMSO)MeCl], may display planar chirality due to the occurrence of the pyridine substituent. The action of the substituent is dual: its presence strongly enhances the rotational barrier around the Pt–N bond, so that the alkyl substituent is located "above" or "below" the coordination plane, hence generating a couple of enantiomers. In addition, the axial Pt···H–C interaction observed in complex **4**, produces a minimum of potential energy which contributes to the stabilization of the chiral conformation.

Experimental Section

Materials: All solvents were purified and dried before use according to standard methods. Dichloromethane-d_2 and benzene-d_6 were used as received from Cortec-Net.

2-ethylpyridine was the highest grade commercially available and was used as received, while 2-vinylpyridine was purified by distillation under reduced pressure. 2-*iso*-propylpyridine and 2-*tert*-butylpyridine were synthesized by cyclo-cotrimerization with acetylene of the corresponding nitriles in the presence of Bonneman catalyst. Selected ^{1}H NMR data of the ligands are given in Table 1.

All the solvents were purified and dried before use according to standard methods.[22] The reactions were performed in air unless otherwise indicated. *trans*-[Pt(Me)Cl($DMSO)_2$] has been synthesized according to literature procedures.[23]

Elemental analyses were performed with a Perkin Elmer elemental analyzer 240B in the Analytical laboratory of our department. Infrared spectra were recorded with FT-IR Jasco 480P or Perkin-Elmer 983 spectrophotometers using Nujol mulls. ^{1}H NMR spectra were recorded at room temperature (20 °C) with a Varian VXR 300 or Bruker Avance III spectrometers operating at 300.0 and 400.1 MHz, respectively. Chemical shifts are given in ppm relative to internal TMS (^{1}H); coupling constants are given in Hz.

Crystallographic method: The crystal data for compound **4** are compiled in Table S1. Crystals of **4** were examined using a Bruker D8 Quest diffractometer with a Photon III detector and a microfocus source with Cu–Kα radiation (λ = 1.54178). A multi-scan absorption correction method with a beam profile was applied.[24] The structures were solved using SHELXT;[25] the datasets were refined by full-matrix least-squares on reflections with $F^2 \geq 2\sigma(F^2)$ values, with anisotropic displacement parameters for all non-hydrogen atoms, and with constrained riding hydrogen geometries;[26] U_{iso}(H) was set at 1.2 (1.5 for methyl groups) times U_{eq} of the parent atom. The largest features in final difference syntheses were close to heavy atoms and were of no chemical significance. SHELX[25,26] was employed through OLEX2 for structure solution and refinement.[27] ORTEP-3[28] and POV-Ray[29] were employed for molecular graphics. The structure has been deposited with the Cambridge Crystallographic Data Centre (CCDC 2298344).

Deposition Number(s) 2298344 (for **4**) contain(s) the supplementary crystallographic data for this paper. These data are provided free of charge by the joint Cambridge Crystallographic Data Centre and Fachinformationszentrum Karlsruhe Access Structures service.

DFT Calculations: Density Functional Theory calculations were carried out using the PBE0 hybrid functional developed by Perdew, Burke and Ernzerhof [30] and modified in its hybrid version by Adamo and Barone,[31] with ZORA[32] using the minimally augmented ma-ZORA-def2-SVP basis set for all atoms except for Pt for which we used a segmented all-electron relativistically contracted (SARC) basis set[33] along with the RI-JONX approximation as implemented in the ORCA 5.0.3 package.[34] Harmonic analysis at the same level of theory was carried out on the equilibrium geometries to confirm the nature of the minimum (*i.e.*, the absence of imaginary frequencies) on the potential energy surface (PES).

Preliminary potential energy surface scans were performed with Firefly QC package,[35] which is partially based on the GAMESS (US)[36] source code.

Images were generated using ORTEP 3[28] and POV-Ray tracer[29]

Experimental Section

Ligands: The ligands 2-*iso*-propylpyridine (py^{ip}) and 2-*tert*-butylpyridine (py^{tb}) were synthesized from the corresponding nitrile (CH-$(CH_3)_2$CN and $C(CH_3)_3$CN, respectively) through co-cyclotrimerization with acetylene in the presence of the cobalt Bonneman catalyst.[13]

2-*iso*-propylpyridine: Yield: 80 %. ^{1}H NMR (300 MHz, CDCl3, 25 °C): δ 8.54 (ddd, [1H], H6) 7.60 (td, [1H], H4), 7.16 (d, [1H], H3), 7.09 (m, [1H], H5), 3.06 (m, [1H], C–H), 1.31 (d, [6H], Me).

2-*tert*-butylpyridine: Yield: 65 %. ^{1}H NMR (300 MHz, CDCl3, 25 °C): δ 8.57 (ddd, [1H], H6) 7.60 (td, [1H], H4), 7.33 (d, [1H], H3), 7.08 (m, [1H], H5), 1.37 (s, [9H], Me).

[Pt(py^R)(DMSO)MeCl] General procedure

To a solution of *trans*-[Pt(Cl)(Me)($DMSO)_2$] (100.0 mg, 0.249 mmol) dissolved in the minimum amount of dichloromethane (10 mL) was added, under stirring at room temperature, a 10 % excess amount of the proper nitrogen ligand. After 2 h, pentane was added

dropwise and the reaction mixture was cooled at −25 °C. The solid precipitate obtained was collected, washed with several small portions of cold pentane and dried under vacuum. The yields were in some cases almost quantitative.

3 *trans*(N,S)-[Pt(py^{Et})(DMSO)MeCl]

Yield: 74%. M.p.: 103 °C. Anal. Calcd for $C_{10}H_{18}ClNOPtS$: C 27.88; H 4.21; N 3.25%. Found: C 27.39, H 3.62, N 3.26%. ^{1}H NMR (C_6D_6): δ 8.41 (ddd, J_{av} 6.6 Hz, ^{3}J Pt–H, 40.7 Hz, 1H), *H6*; 6.67 (td, $J_{H–H}$ 1.5, $J_{H–H}$ 7.7, 1H), *H4*; 6.44 (d br, $J_{H–H}$ 7.3, 1H), *H3*; 6.11(m, $J_{H–H}$ 7.3, 1H), *H5*; 3.52 (m, 1H) MeCH_aH$_b$; 3.36 (m, 1H) MeCH$_a$$H_b$; 3.15 (s, $^3J_{PtH}$ 27.1 Hz, 3H) *Me*MeSO; 3.11 (s, $^3J_{PtH}$ 26.4 Hz, 3H) Me*Me*SO; 1.24 (s, $^3J_{PtH}$ 82.5 Hz, 3H) *Me*Pt; 1.17 (t, $J_{H–H}$ 7.7 Hz, 3H) *Me*CH$_2$. ^{1}H NMR (CD_2Cl_2): δ 8.62 (ddd, J_{av} = 5.0 Hz, ^{3}J Pt–H, 40.8 Hz, 1H), *H6*; 7.80 (td, $J_{H–H}$ 1.5 Hz, $J_{H–H}$ 7.5 Hz, 1H), *H4*; 7.41 (td, $^4J_{Pt–H}$ 14.5 Hz, $J_{H–H}$ 7.5 Hz, 1H), *H3*; 7.27 (tm, $J_{H–H}$ 6.2 Hz, 1H), *H5*; 3.48 (m, 2H) Me*CH$_2$*; 3.44 (s, $^3J_{Pt–H}$ 35.40 Hz, 6H) *MeMe*SO; 1.41 (t, $^3J_{H–H}$ 7.1 Hz, 3H) *Me*CH$_2$; 0.65 (s, $^2J_{Pt–H}$ 83.9 Hz, 3H) *Me*Pt.

4 *trans*(N,S)-[Pt(py^{ip})(DMSO)MeCl]

Yield: 80%. M.p.: dec. 150 °C. Anal. Calcd for $C_{11}H_{20}ClNOPtS$: C 29.70; H 4.53 ; N 3.15%. Found: C 29.72, H 4.16, N 3.18%. ^{1}H NMR(C_6D_6): δ 8.37 (ddd, J_{av} 5.8 Hz, $^3J_{Pt–H}$, 40.7 Hz, 1H), *H6*; 6.68 (t br, $J_{H–H}$ 7.4, 1H), *H4*; 6.52 (d br, $J_{H–H}$ 7.2, 1H), *H3*; 6.17 (t br, $J_{H–H}$ 7.4, 1H), *H5*; 4.77 (m, 1H) MeMe*CH*; 3.09 (s, $^3J_{PtH}$ 26.8 Hz, 3H) *Me*MeSO; 3.05 (s, $^3J_{PtH}$ 26.3 Hz, 3H) Me*Me*SO; 1.33 (d, $J_{H–H}$ 6.8 Hz, 3H) Me*Me*CH; 1.22 (s, $^2J_{Pt–H}$ 82.7 Hz, 3H) *Me*Pt; 1.06 (t, $J_{H–H}$ 7.0 Hz, 3H) *Me*MeCH. ^{1}H NMR (CD_2Cl_2): δ 8.60 (ddd, J_{av} 5.8 Hz, $^3J_{Pt–H}$, 42.16 Hz, 1H), *H6*; 7.82 (td, $J_{H–H}$ 1.6 Hz, $J_{H–H}$ 7.5 Hz, 1H), *H4*; 6.44 (d br, $^4J_{Pt–H}$ 21.7 Hz, $J_{H–H}$ 7.6 Hz, 1H), *H3*; 7.3(ddd $J_{H–H}$ 1.6 Hz, $J_{H–H}$ 5.9 Hz, $J_{H–H}$ 7.4 Hz, 1H), *H5*; 4.49 (m, 1H) MeMe*H*; 3.44 (s, $^3J_{PtH}$ 2.1 Hz, 3H) Me*Me*SO; 1.39 (t, $J_{H–H}$ 6.8 Hz, 3H) *Me*MeCH; 1.33 (d, $J_{H–H}$ 7.0 Hz, 3H) *Me*MeCH; 0.65 (s, $^2J_{PtH}$ 83.5 Hz, 3H) *Me*Pt.

5 *trans*(N,S)-[Pt(py^{tb})(DMSO)MeCl]

Complex **5** was not isolated in pure form, but only in mixture with the starting complex [Pt(DMSO)$_2$MeCl].

^{1}H NMR (300 MHz, CD_2Cl_2, 25 °C): δ 9.16 (ddd, [1H], H6, $^3J_{Pt–H}$ = 38.7 Hz), 7.78 (td, [1H], H4), 7.68 (d br, [1H], H3), 7.23 (m, [1H], H5), 3.47 (s, [6H], Me (DMSO), $^3J_{Pt–H}$ = 26.2 Hz), $^3J_{Pt–H}$ = 24.4 Hz), 1.78 (s, [9H], CH_3 tert-butyl), 0.66 (s, [3H], Pt–CH_3, $^2J_{PtH}$ = 84.9 Hz).

6 *trans*(N,S)-[Pt(py^{np})(DMSO)MeCl]

Yield: 88%. M.p. = dec. 100 °C. Anal. Calcd for $C_{13}H_{24}ClNOPtS$: C 33.02%, H 5.12%, N 2.96%; found: C 32.89%, H 4.55%, N 2.96%. ^{1}H NMR (300 MHz, $CDCl_3$, 25 °C): δ 8.72 (ddd, [1H], H6, $^3J_{Pt–H}$ = 41.5 Hz), 7.77 (td, [1H], H4), 7.41 (d br, [1H], H3, $^4J_{Pt–H}$ = 12.1 Hz), 7.30 (m, [1H], H5), 3.71 (d, [1H], CH_2 neopentyl), 3.53 (s, [3H], Me(DMSO), $^3J_{Pt–H}$ = 26.3 Hz), 3.50 (s, [3H], Me (DMSO), $^3J_{Pt–H}$ = 26.7 Hz), 3.30 (d, [1H], CH_2 neopentyl), 1.08 (s, [9H], Me neopentyl), 0.78 (s, [3H], Pt–CH_3, $^2J_{Pt–H}$ = 83.8 Hz).

7 *trans*(N,S)-[Pt(py^{vi})(DMSO)MeCl]

Yield: 75%. M.p. = 96–98 °C. Anal. Calcd for $C_{10}H_{16}ClNOPtS$: C 28.01%, H 3.76%, N 3.27%; found: C 27.89%, H 3.49%, N 3.19%. ^{1}H NMR (300 MHz, CD2Cl2, 25 °C): δ 8.69 (ddd, [1H], H6, JH–H = 5.8 Hz, $^3J_{Pt–H}$ = 42.2 Hz), 7.99 (m, [1H], CHACHMHX, $J_{H–H(cis)}$ = 11.1 Hz, $J_{H–H(trans)}$ = 17.5 Hz, $J_{Pt–H}$ = 11.3 Hz), 7.9 (t, [1H], H4, $J_{H–H}$ = 8.3 Hz), 7.8 (d, [1H], H3, $^4J_{Pt–H}$ = 14 Hz ca., $J_{H–H}$ = 7.1 Hz), 7.3 (t, [1H], H5, $J_{H–H}$ = 7.1 Hz), 6.05 (d, [1H], $CH_ACH_MH_X$, $J_{H–H(trans)}$ = 17.6 Hz), 5.79 (d, [1H], $CH_ACH_MH_X$, $J_{H–H(cis)}$ = 11.1 Hz), 3.47 (s, [3H], Me (DMSO), $^3J_{Pt–H}$ = 27.2 Hz), 3.45 (s, [3H], Me (DMSO), $^3J_{Pt–H}$ = 25.6 Hz), 0.63 (s, [3H], Pt–CH3, 2JPt–H = 83.6 Hz).

A series of Pt(II) complexes with 2-alkylsubstituted pyridines display planar chirality due to the influence of the pyridine substituent, which enhances the rotational barrier around the Pt–N bond generating a couple of enantiomers. The chiral conformation is also stabilized by the presence of an axial Pt···H–C interaction.

Conflict of Interests

The authors declare no conflict of interest.

Data Availability Statement

The data that support the findings of this study are available from the corresponding author upon reasonable request.

Keywords: chiral complexes · metal-hydrogen interactions · N-ligands · platinum · pyridine complexes

[1] a) A. Sliwa, *Transition Met. Chem.* **1995**, *20*, 1–12; b) *Comprehensive Coordination Chemistry II, Vol. 6, Transition Metal Groups 9–12*, Edited by D. E. Fenton, T. J., Ed. A. B.P Level, Elsevier, Amsterdam, **2003**.
[2] U. Belluco, L. Cattalini, F. Basolo, R. G. Pearson, A. Turco, *J. Am. Chem. Soc.* **1965**, *87*, 241–246.
[3] S. Huo, J. Carroll, D. A. K. Vezzu, *Asian J. Org. Chem.* **2015**, *4*, 1210–1245.
[4] T. C. Johnstone, P. M. Pil, S. J. Lippard, *Cisplatin and Related Drugs, Reference Module in Biomedical Sciences* Elsevier Inc., **2015**, 1–14.
[5] R. Romeo, L. Monsù Scolaro, N. Nastasi, B. E. Mann, G. Bruno, F. Nicolò, *Inorg. Chem.* **1996**, *35*, 7691–7698.
[6] L. Monsù Scolaro, A. Mazzaglia, A. Romeo, M. R. Plutino, C. Castriciano, R. Romeo, *Inorg. Chim. Acta* **2002**, *330*, 189–196.
[7] A. von Zelewsky, *Platinum Met. Rev.* **1996**, *40*, 102–109.
[8] H. Amouri, M. Gruselle, *Chirality in Transition Metal Chemistry: Molecules, Supramolecular Assemblies and Materials* John Wiley and sons, U. K., **2008**.
[9] M. C. Biagini, M. Ferrari, M. Lanfranchi, L. Marchiò, M. A. Pellinghelli, *J. Chem. Soc. Dalton Trans.* **1999**, 1575–1580.
[10] a) A. Zucca, D. Cordeschi, S. Stoccoro, M. A. Cinellu, G. Minghetti, G. Chelucci, M. Manassero, *Organometallics* **2011**, *30*, 3064–3074; b) S. Stoccoro, G. Minghetti, A. Zucca, M. A. Cinellu, M. Manassero, S. Gladiali, *Inorg. Chim. Acta* **2006**, *359*, 1879–1888; c) M. A. Cinellu, A. Zucca, S. Stoccoro, G. Minghetti, M. Manassero, M. Sansoni, *J. Chem. Soc. Dalton Trans.* **1995**, 2865–2872; d) G. Minghetti, A. Zucca, S. Stoccoro, M. A. Cinellu, M. Manassero, M. Sansoni, *J. Organomet. Chem.* **1994**, *481*, 195–204.
[11] a) L. Maidich, G. Dettori, S. Stoccoro, M. A. Cinellu, J. P. Rourke, A. Zucca, *Organometallics* **2015**, *34*, 817–828; b) V. G. Albano, C. Castellari, M. Monari, V. de Felice, A. Panunzi, F. Ruffo, *Organometallics* **1996**, *15*, 4012–4019; c) G. R. Newkome, D. C. Pantaleo, W. E. Puckett, P. L. Ziefle, W. A. Deutsch, *W.A.J. Inorg. and Nucl. Chem.* **1981**, *43*, 1529–1531; d) A. Doppiu, M. A. Cinellu, G. Minghetti, S. Stoccoro, A. Zucca, M. Manassero, M. Sansoni, *Eur. J. Inorg. Chem.* **2000**, 2555–2563.
[12] A. Zucca, S. Stoccoro, M. A. Cinellu, G. L. Petretto, G. Minghetti, *Organometallics* **2007**, *26*, 5621–5626.
[13] H. Bonnemann, *Angew. Chem. Int. Ed.* **1985**, *24*, 248–262.
[14] R. Romeo, L. Monsù Scolaro, V. Catalano, S. Achar, *Inorganic Syntheses* Volume 32, Ed. by M. York Darensbourgh, John Wiley and Sons, **1998**, *32*, 153–157.
[15] E. A. Baquero, A. Rodríguez-Zúñiga, J. C. Flores, M. Temprado, E. de Jesús, *J. Organomet. Chem.* **2019**, *896*, 108–112.

[16] A. Zucca, L. Maidich, V. Carta, G. P. Petretto, S. Stoccoro, M. A. Cinellu, M. I. Pilo, G. J. Clarkson, *Eur. J. Inorg. Chem.* **2014**, 2278–2287.
[17] a) C. M. Ong, T. J. Burchell, R. J. Puddephatt, *Organometallics* **2004**, *23*, 1493–1495; b) V. G. Albano, D. Braga, V. De Felice, A. Panunzi, A. Vitagliano, *Organometallics* **1987**, *6*, 517–525; c) S. Pischedda, S. Stoccoro, A. Zucca, G. Sciortino, F. Ortu, G. J. Clarkson, *Dalton Trans.* **2021**, *50*, 4859–4873; d) M. Azizpoor Fard, A. Behnia, R. J. Puddephatt, *Organometalics* **2018**, *37*, 3368–3377.
[18] A. Abo-Amer, P. D. Boyle, R. J. Puddephatt, *Inorg. Chim. Acta* **2021**, *522*, 120387.
[19] a) E. Wehman, G. Van Koten, C. T. Knapp, H. Ossor, M. Pfeffer, A. L. Spek, *Inorg. Chem.* **1988**, *27*, 4409–4417; b) O. F. Wendt, Å. Oskarsson, J. G. Leipoldt, L. I. Elding, *Inorg. Chem.* **1997**, *36*, 4514–4519; c) P. Kapoorm, V. Y. Kukushkin, K. Lövqvist, Å. Oskarsson, *J. Organomet. Chem.* **1996**, *517*, 71–79.
[20] W. Scherer, A. C. Dunbar, J. E. Barquera-Lozada, D. Schmitz, G. Eickerling, D. Kratzert, D. Stalke, A. Lanza, P. Macchi, N. P. M. Casati, J. Ebad-Allah, C. Kuntscher, *Angew. Chem. Int. Ed.* **2015**, *54*, 2505–2509.
[21] J. Echeverrìa, S. Alvarez, *Chem. Sci.* **2023**, doi 10.1039/d3sc02238b.
[22] a) D. D. Perrin, W. L. F. Armarego, *Purification of Laboratory Chemicals* 3rd ed., Pergamon Press, Oxford, **1988**; b) A. I. Vogel, *Vogel's Textbook of Practical Organic Chemistry* Longman Scientific & Technical Ed., 5th ed., Harlow, **1989**.
[23] C. Eaborn, K. Kundu, A. J. J. Pidcock, *J. Chem. Soc. Dalton Trans.* **1981**, 933.
[24] G. M. Sheldrick, *Program for Area Detector Absorption Correction* Institute for Inorganic Chemistry, University of Göttingen: Göttingen, Germany, **1996**.
[25] G. M. Sheldrick, *Acta Crystallogr. Sect. C.* **2015**, *71*, 3–8.
[26] G. M. Sheldrick, *Acta Crystallogr. Sect. A.* **2008**, *64*, 112–122.
[27] O. V. Dolomanov, L. J. Bourhis, R. J. Gildea, J. A. K. Howard, H. Puschmann, *J. Appl. Crystallogr.* **2009**, *42*, 339–341.
[28] L. J. Farrugia, *J. Appl. Crystallogr.* **2012**, *45*, 849–854.
[29] *POV-Ray*, Persistence of Vision Raytracer Pty. Ltd.: Williamstown, Australia, **2013**.
[30] a) J. P. Perdew, K. Burke, M. Ernzerhof, *Phys. Rev. Lett.* **1996**, *77*, 3865–3868; b) J. P. Perdew, K. Burke, M. Ernzerhof, *Phys. Rev. Lett.* **1997**, *78*, 1396–1396.
[31] C. Adamo, V. Barone, *J. Chem. Phys.* **1999**, *110*, 6158–6170.
[32] a) E. van Lenthe, E. J. Baerends, J. G. Snijders, *J. Chem. Phys.* **1993**, *99*, 4597–4610; b) C. Chang, M. Pelissier, P. Durand, *Phys. Scr.* **1986**, *34*, 394–404; c) J. L. Heully, I. Lindgren, E. Lindroth, S. Lundqvist, A. M. Martensson-Pendrill, *J. Phys. B: At. Mol. Phys.* **1986**, *19*, 2799–2815;d) E. van Lenthe, A. Ehlers, E.-J. Baerends, *J. Chem. Phys.* **1999**, *110*, 8943–8953.
[33] D. A. Pantazis, X.-Y. Chen, C. R. Landis, F. Neese, *J. Chem. Theory Comput.* **2008**, *4*, 908–919.
[34] a) F. Neese, *Comput. Mol. Sci.* **2012**, *2*, 73–78; b) F. Neese, *Comput. Mol. Sci.* **2018**, *8*, e1327.
[35] Alex A. Granovsky, Firefly version 8, http://classic.chem.msu.su/gran/firefly/index.html.
[36] M. W. Schmidt, K. K. Baldridge, J. A. Boatz, S. T. Elbert, M. S. Gordon, J. H. Jensen, S. Koseki, N. Matsunaga, K. A. Nguyen, S. Su, T. L. Windus, M. Dupuis, J. A. Montgomery, *J. Comput. Chem.* **1993**, *14*, 1347–1363.

Manuscript received: November 7, 2023
Revised manuscript received: November 19, 2023
Accepted manuscript online: November 22, 2023
Version of record online: December 6, 2023